Numerical Study Of Coated Electrical Contacts

Per Lindholm
Machine Design KTH
Brinellvägen 83
SE-10044 Stockholm
per@md.kth.se

Abstract: Electrical contacts consists of parts where the surfaces are in contact and where the actual physical contact occur just in a few contact asperity points scattered over the whole apparent contact area. Through these contact spots between the two mating bodies the mechanical load and the electric current is transmitted. Often a soft coating is used to enlarge the real contact area. Modeling the mechanical stress on the contacting material includes nonlinear effects of the electric conduction and heat generation as well as the actual mechanical contact of the asperities. COMSOL Multiphysics has been used to model these thermo electromechanical phenomena when two surface asperities are in contact.

Keywords: Electrical contacts,

1. Introduction

The contact mechanics of electrical contacts has been well investigated by many researchers during the last decades [1,2,3]. The physical aspects on the phenomena involved in the transfer of electricity over a contact interface includes advanced knowledge in mechanics, materials and physics. Nonlinear effects as the contact itself and material properties that changes with the amount of current and temperature in the contact makes it difficult to investigate and simulate.

Surge arresters are protective devices on the grid which consists of semi conductive zinc oxide (ZnO) blocks stapled together in a stack and pretension via glass fiber loops [4,5]. They are coated with aluminum coating to improve the current capability and give good contact between the blocks. Figure 1 show such a block combination in contact indicating the contact spots occurring when two rough surfaces are in contact [6,7].

Previous work [8] has shown the increase in temperature due to the joule heating effect for different material combinations. This work adds the structural mechanics to the solution and examines the material combination relevant in the surge arrester case.

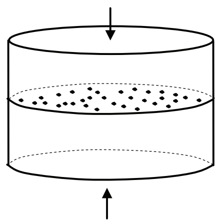

Figure 1. Schematic view of the contact spot formation when two rough surfaces are in contact.

This paper presents a numerical study of an asperity in contact with the influence of coating thickness to the amount of transferred current in the contact.

2. Theory

In a stationary electrical contact the contact members are connected by a pretension mechanical load to physically connect the members together. The mechanical load F is carried by the asperities in contact. The size of the mechanical contact A_a can be described by the relationship between the hardness H and the load.

$$A = \frac{F}{H} \qquad (1)$$

However the actual size of the contact spot the a-spot that transfers the current is just a fraction of the mechanical loaded spot. The size depends mainly on the oxide layer and other impurities which covers the metallic contact surface. Holm [1] has shown that the constriction resistance R_s with the same metal resistivity ρ on both members can be calculated as:

$$R_s = \rho/2a \qquad (2)$$

The multiphysics problem consists of solving a combination of structural mechanic problem, heat transfer and the electric current field.

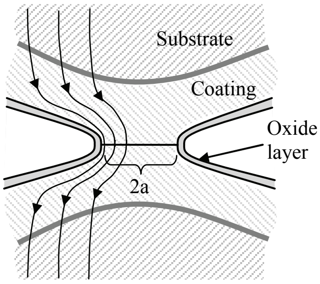

Figure 2. Schematic figure of the coated contact asperity with oxide layer and the current paths indicated.

In reality the surface asperities come into contact and a contact definition between the surfaces would be needed in solving the complete problem. However this has shown to be very sensitive and hard to solve when the joule heating part is added. Therefore a simplification has been done where the Hertzian contact pressure distribution is used as mechanical load. Previous work by the author [8,9] has used a similar approach in a completely different application. At the contact interface between a spherical indenter and an opposite surface the pressure distribution can be calculated according to the Hertz equation from [7]:

$$p(r) = p_{\max}\sqrt{1-\frac{r^2}{a^2}} \qquad (3)$$

for all r<a, a is the contact radius of the Hertzian contact.

The temperature dependence, T, of the electric conductivity can be described by the following equation:

$$\sigma = \frac{1}{\rho_0\left(1+\alpha\left(T-T_{ref}\right)\right)} \qquad (4)$$

where ρ_0 is the resistivity at the reference temperature T_{ref} and α is the resistivity temperature coefficient.

5. Numerical model

The Comsol 4.0 model is defined as a Joule Heating and Thermal Expansion multiphysics model. The special case for axisymmetry is used and the conditions for stationary conditions is calculated. A thermal linear elastic material model is used.

Parameterization:

The Comsol capability of parameterization has been used where all the parameters are defined in the global parameter definition.

Table 1. Parameters used in the model (setup values).

Name	Expression	Description
B	50[µm]	Model width
H	100[µm]	Model height
Rc	14[µm]	Contact radius
ct	4[µm]	Coating thickness
a	4[µm]	a-spot diameter
I0	4[A]	Current
Am	pi*B^2	Model cross section
J0	I0/Am	Current density
p0	200[MPa]	Maximum Hertzian pressure
mt	1[µm]	Element size

Table 2. Variable used in the model.

Name	Expression	Description
pn	p0*sqrt(1-r^2/Rc^2)	Contact pressure distribution

Geometry:

The geometry is defined from the parameters into a single part. The part is divided in an a-spot part, size a, where the current and heat is transferred and a load carrying part, size Rc, where the load is defined. A coating thickness ct defines the thickness of the coating material. Figure 3 shows the geometry with the used geometrical parameters.

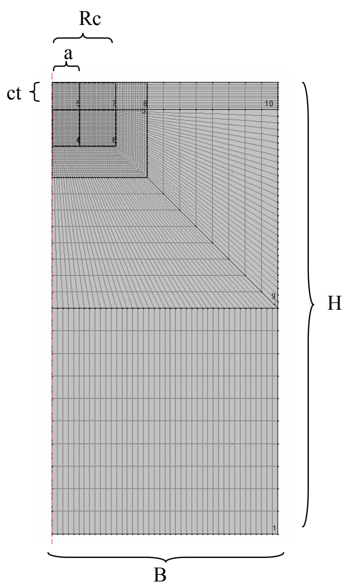

Figure 3. Geometry of the Comsol model

Electrical boundary conditions:
On the vertical right outer boundary and on the top surface from the a-spot radius to the outer end electrical insulation is defined, that is no electrical current is passed over the surface.

$$n \cdot J = 0$$

The top surface over the distance a on the a-spot is grounded and on the bottom surface a normal current density is applied as the electrical load on the model.

Heat transfer boundary condition:
The outer boundaries same as for the electrical case is thermally insulated that is the heat flux over the surface is zero.

$$n \cdot \left(k\nabla T\right) = 0$$

The temperature on the top and bottom boundaries are set to 293K..

Mechanical boundary condition:
The bottom boundary as well as the right vertical boundary have roller constraints that means the motion in the direction normal to the surface is constrained but it is free to move in the tangential direction of the surface.

Mesh:
The mesh is defined as a mapped mesh with a fixed element size close to the a-spot and the load area of the parameter mt µm. Quadratic elements are used.

Material properties used in the calculations for each combination is shown in table 2. The substrate has similar material a ZnO which is a semiconductor with nonlinear resistivity depending on the voltage across the specimen [4,5].

Table 3. Properties of the material data used in the model collected from [2] and [5].

Property	Substrate	Coating
Young´s modulus [GPa]	113	70
Poisson´s ratio [-]	0.35	0.33
Density [kg/m^3]	5600	2700
Coefficient of thermal expansion [1/K]	6.6e-6	2.3e-5
Relative permittivity [-]	1	1
Thermal conductivity [W/(mK]	10	222
Heat capacity at constant pressure [(J/(kgK))]	540	896
Reference resistivity [Ωm]	3e-8	2.65e-8
Resistivity temperature coefficient [1/K]	1e-9	4.6e-3
Reference temperature [K]	293	293
Meltingpoint [^{o}C]		660
Hardness [N/mm^2]		200

6. Experimental results

The results consist of a study of the parameters in the model. First a study of the application of the load and then increasing the current over the asperity from the nominal parameter data set up. Figure 4 shows the stress deformation under load from a spherical indent at no current. Figure 5 then shows the Tresca-shear stress at increasing current passing through the a-spot constriction.

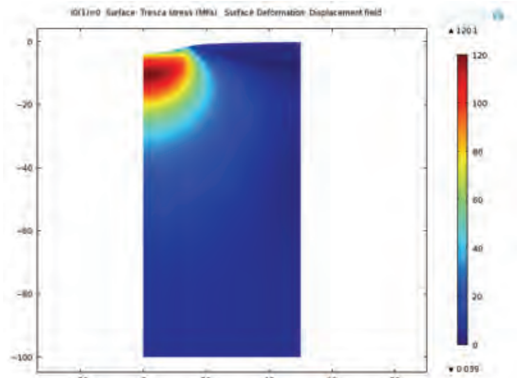

Figure 4. Model under pressure load and I=0A. Maximum shear stress [MPa]. Deformation scale 100.

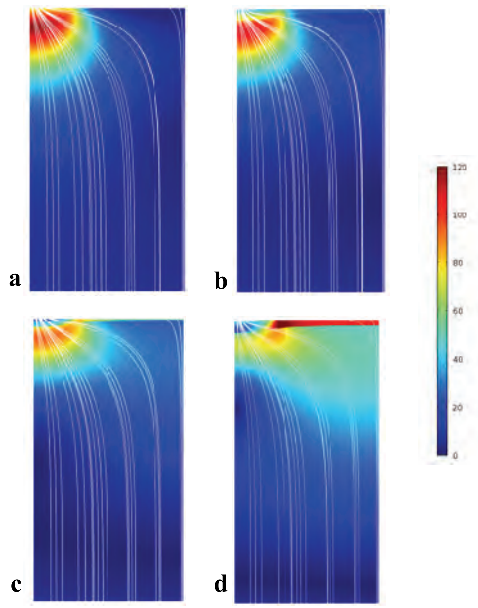

Figure 5. Model under pressure load and the current through the a spot is increased in a J_n=0A, b J_n =1A, c J_n =3A and in d J_n =4A. Current density streamlines is also indicated in the figures.

When the current is increased the temperature also increases as resistive heating in the constriction a-spot. Figure 6,7 and 8 show the temperature development up to the melting temperature of the coating and in figure 7 the voltage drop over the contact.

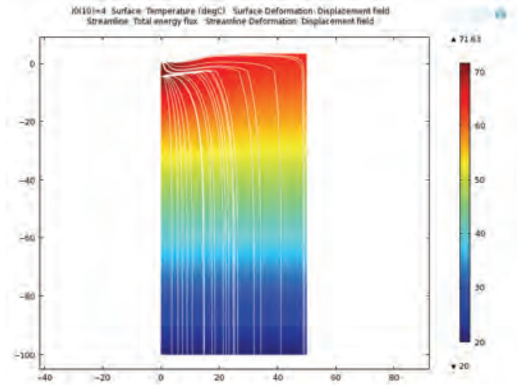

Figure 6. Temperature [^{o}C] in the model at J_n =4A. Streamlines show the energy flux. Deformations are scaled 100 times.

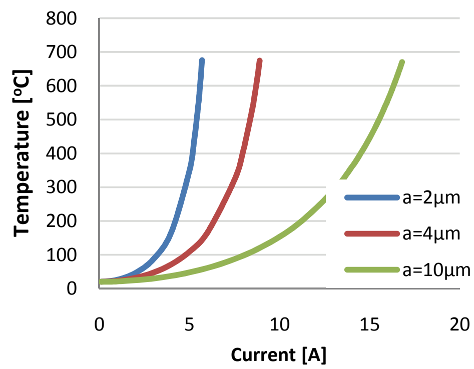

Figure 7. Maximum temperature in the model for different a-spot sizes as a function of current passing through the contact.

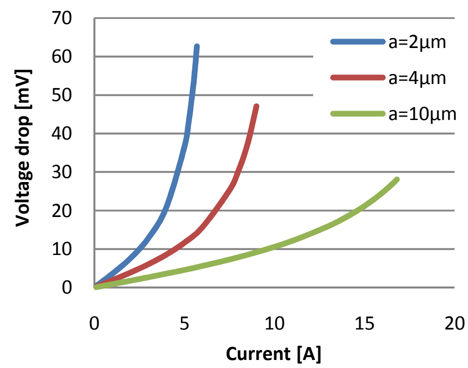

Figure 8. Voltage drop over the contact a-spot

From the initial state defined in table 1 the coating thickness is varied from 2-12µm. Figure 9 show the maximum temperature development in the model due to a change in coating thickness at the same applied current density. In figure 9 the maximum shear stress (Tresca stress) is shown on the boundary between the coating and the substrate for different coating thicknesses.

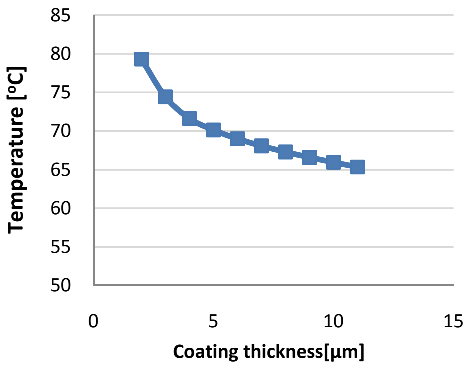

Figure 9. Maximum temperature in the model for different coating thicknesses.

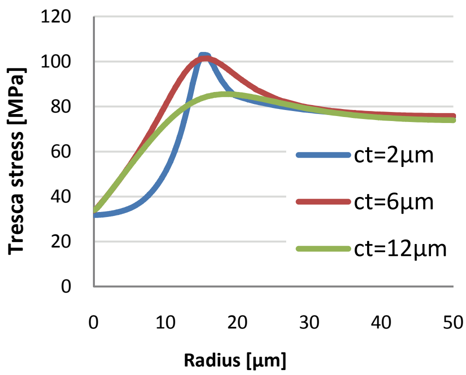

Figure 9. Tresca shear stress in the interface of substrate and coating for different coating thicknesses.

7. Discussion

Modeling an electrical contact combines several physics into the same simulation. Comsol has shown to have the capability of combining these areas. In this work several modeling approaches were tested. A contact model was analyzed but the solver had problems finding a solution when the combined multiphysics was simulated also a segregated multiphysics contact solution was investigated. Problems with defining pairs and ease to have a flexible model investigating different parameters pointed towards the chosen solution. Another way to investigate the effect of joule heating in the asperity is to used the whole geometry as shown in figure 2 and use the contact resistant functionality at suitable boundaries defining the a-spot and the resistive oxide layer. However the pretension load from the outer clamping force is then hard to accomplish.

In this simulation temperatures spread out rapidly in the coating due to the much lower conductivity of the coating in relation to the substrate. The shear stress maxima shifts upward towards the surface due to a thermal expansion of the complete structure.

Coating thickness reduces maximum temperature and evens out shear stresses in the interface to the substrate.

Future work would be to investigate the effect of a elastoplastic material model

8. Conclusion

The work show a possible way to simulate the combined deformation and resistive heating problem in an electrical contact. It gives a illustrative and easy way of investigating the effects of coating thickness, a-spot size, contact load and size.

9. References

1. R. Holm, Electrical Contacts - Theory and Applications, 4th Ed., Springer-Verlag, Berlin 1967
2. P.G.Slade, Electrical Contacts - Principles and Applications, Marcel Dekker, New York 1999
3. M.Braunovic´, V. Konchits, N.Myshkin, Electrical Contacts - Fundamentals, Application and Technology, CRC Press Taylor Francis Group, 2007
4. Mobedjina M. Jonnerfelt B., Stenström L., Design and testing of polymer-housed surge arresters, GCC CIGRÉ 9th Symposium, Abu Dabi, 1998
5. Haddad A., Warne D.F., Advances in High Voltage Engineering, The Institution of Electrical Engineers, London, UK, 2004
6. T.R. Thomas, Rough Surfaces, 2nd Ed. Imperial College Press, London
7. Johnsson K.L., Contact Mechanics, Cambridge University Press, 1985
8. Å. Öberg, K.E. Olsson, O.Saksvik, Computer simulation of the electrical and thermal behaviour of electrical contacts, Proc 17th Int. Conf. on Electrical Contacts, 1994, pp 785-792.
9. Lindolm P., Björklund S., Svahn F., Method and surface roughness aspects for the design of DLC coatings, 2006 Wear 261 (1), pp. 107-111
10. Lindholm P., Svahn F., Study of thickness dependence of sputtered carbon coating for low friction valve lifters, 2006, Wear 261 (3-4), pp. 241-250

9. Acknowledgements

This work was supported by the Swedish Foundation for Strategic Research